Thermochimica Acta, 183 (1991) 1–14
Elsevier Science Publishers B.V., Amsterdam

Heat capacity measurement of $VO_{1\pm x}$ and niobium doped VO_{1+x} [α]

Tsuneo Matsui, Toshihide Tsuji, Takashi Asano[1] and Keiji Naito

Department of Nuclear Engineering, Faculty of Engineering, Nagoya University, Furo-cho, Chikusa-ku, Nagoya 464-01 (Japan)

(Received 6 June 1990)

Abstract

The heat capacities of $VO_{1\pm x}$ (O/V = 0.883 and 1.063 (δ-phase) and 1.267 (ε-phase) were measured in the temperature range of 324–920 K with an adiabatic scanning calorimeter. A steep decrease in the heat capacity near room temperature and a subsequent anomalous peak were observed for each sample in the low temperature range below 600 K. At high temperature, around 900 K, an anomalous peak was seen in $VO_{0.883}$ and $VO_{1.063}$. The high temperature heat capacity peak was thought to be due to the order–disorder rearrangement of clusters of oxygen and vanadium vacancies and/or clusters of interstitial vanadium and vanadium vacancies. The low temperature heat capacity anomaly was interpreted by atomic migration to induce an increase in the degree of order of the "frozen in" state at some higher temperature. The heat capacities of VO_{1+x} doped with 1.6 and 30 at% of Nb were also measured in the same temperature range, and the results supported the presence of the similar order–disorder transition to undoped $VO_{1\pm x}$ at high temperature. The enthalpy and entropy changes at the high temperature transition were calculated from the excess heat capacity. The entropy change at the transition obtained experimentally was compared with that calculated from the configurational change of the two types of defect clusters mentioned above. The electrical conductivities of $VO_{1.063}$ and $VO_{1.267}$ were measured in the temperature range 320–1200 K. The δ-$VO_{1\pm x}$ phase ($VO_{1.063}$) was observed to be semiconducting and the slope in the conductivity curve changed around the peak temperatures of low and high heat capacity anomalies. The ε-VO_{1+x} phase ($VO_{1.267}$) was a metallic conductor and the slope in the conductivity of $VO_{1.267}$ changed slightly near the peak temperature of the low temperature heat capacity anomaly.

INTRODUCTION

Vanadium monoxide has a wide homogeneity range on the sides of both hypo- and hyperstoichiometry, and is known to contain large numbers of

[α] Paper presented at the Second Japan–China Joint Symposium on Calorimetry and Thermal Analysis, 30 May–1 June 1990, Osaka, Japan.

[1] Present address; Energy Research Laboratory, Hitachi, Ltd., Hitachi-shi, Ibaraki-ken, 316, Japan

0040-6031/91/$03.50

interstitial vanadium ions and vacant sites in both anion and cation sublattices [1–6]. For example, even at the stoichiometric composition $VO_{1.000}$, about 15.2 at% of each type of sublattice is vacant and the composition may therefore be written in the form $(VO)_{0.848}(V_vO_v)_{0.152}$, where V_v and O_v are a vanadium vacancy and oxygen vacancy, respectively [1]. The local distribution of vacancies in $VO_{1\pm x}$ has been studied by several investigators [1–6]. By using X-ray and electron diffractometry, Saeki and Nakahira [2] revealed the presence of a tetragonal phase in the range between $x = 0.15$ and 0.25 in addition to the cubic $VO_{1\pm x}$ phase and also a superstructure consisting of cation vacancy clusters in the tetragonal phase. Andersson et al. [3] showed by electron diffractometry two types of defect clusters: the interstitial vanadium ion–vanadium vacancy tetrahedron in the hyperstoichiometric tetragonal $VO_{1.20}$ and a cluster of oxygen vacancies associated with displacement of vanadium ions in the hypostoichiometric cubic $VO_{0.9}$. Morinaga and Cohen [4,5] determined the defect structure of $VO_{1\pm x}$ by X-ray diffuse scattering analysis and proposed the presence of the same clusters, composed of the interstitial vanadium ion–vanadium vacancy tetrahedron in the hyperstoichiometric region, as proposed by Andersson et al. [3], and the clusters of oxygen and vanadium vacancies in the hypostoichiometric region. The order–disorder transition due to the displacement of the oxygen ions around an interstitial vanadium ion by a long-range cooperative interaction among them has also been reported in the hyperstoichiometric tetragonal phase VO_{1+x} ($x = 0.2$–0.3) by Morinaga and Cohen [4] and Andersson and Gjönnes [6]. However there has been no report on the presence of the order–disorder transition in cubic $VO_{1\pm x}$ ($x < 0.20$).

The heat capacity of $VO_{1\pm x}$ has been measured by several investigators [7–9]. Todd and Bonnickson [7] measured the heat capacity of VO in the temperature range of 55–298 K by the adiabatic method. Chernyaev et al. [8] also determined the heat capacities of $VO_{1\pm x}$ with various compositions (O/V = 0.86, 0.99, 1.24 and 1.30) in the range 60–300 K by the adiabatic method. The heat capacity of $VO_{0.99}$ reported by Chernyaev et al. is considerably lower than that of VO (O/V $\approx$ 1.0) reported by Todd and Bonnickson. Orr [9] used the same sample of VO as Todd and Bonnickson and determined the heat capacity in the higher temperature range of 298–1698 K from the enthalpy values obtained by the drop method. The heat capacity reported by Orr showed a smooth sequence to that obtained by Todd at 298 K.

In this paper, the heat capacities of $VO_{1\pm x}$ (O/V = 0.883, 1.063 and 1.267) were measured in the temperature range of 324–920 K with an adiabatic scanning calorimeter to determine the compositional dependence of the heat capacity and the phase stability of the cubic and tetragonal phases. The heat capacity of VO_{1+x} doped with Nb and the electrical conductivities of $VO_{1.063}$ and $VO_{1.267}$ were also measured in order to estimate the origin of the heat capacity anomaly observed in $VO_{1\pm x}$ in this study.

EXPERIMENTAL

Sample preparation

Vanadium metal powder and V_2O_3 powder were used for the preparation of the $VO_{1\pm x}$ samples. The purity of the vanadium metal powder was higher than 99.99%. The V_2O_3 powder was prepared by reducing V_2O_5 powder, of purity higher than 99.99%, at 873 K for 6 h and then at 1173 K for 18 h in a hydrogen gas stream. The appropriate amounts of V metal and V_2O_3 powders were mixed and pressed into pellets. For the preparation of the sample buttons of VO_{1+x} doped with Nb, niobium metal (purity > 99.99%), V metal and V_2O_3 powders were mixed and pressed into pellets. The pellets thus prepared for $VO_{1\pm x}$ and $(V,Nb)O_{1+x}$ were melted several times using an Ar plasma jet furnace. Sample buttons made in the plasma jet furnace were annealed at 1173 K for one week in evacuated and sealed quartz tubes, and then cooled down to room temperature over a period of one week. The annealed button was then crushed into pieces less than 3 mm in size using a stainless-steel mortar, and then sealed in a small quartz vessel for the heat capacity measurements.

The pellets of $VO_{1.063}$ and $VO_{1.267}$ for the electrical conductivity measurements were prepared as follows [11]. The mixture of V and V_2O_3 powders was pressed into pellets in a circular die at about 400 MPa. Four holes 0.3 mm in diameter were drilled in a line and a platinum wire 0.3 mm in diameter was inserted into each hole in the pellet as an electrode. The pellets with platinum electrodes were sintered in the evacuated and sealed quartz tubes at 1223 K for 72 h and cooled to room temperature over a period of one week. The pellets thus prepared were about 10 mm in diameter and 2 mm in thickness. The electrical conductivity measurement was carried out in a sealed quartz glass tube to avoid compositional change during the measurements.

The O/V ratios of $VO_{1\pm x}$ and $(V,Nb)O_{1+x}$ samples were determined from the weight gain of the samples after oxidizing them to V_2O_5 and

TABLE 1

Composition and phase of sample

Compound	O/V ratio	Nb/(V+Nb) ratio	Phase
$VO_{1\pm x}$	0.883 ± 0.004		δ-VO (cubic)
	1.063 ± 0.002		δ-VO (cubic)
	1.267 ± 0.002		ϵ-VO (tetragonal)
$(V, Nb)O_{1+x}$	1.02 ± 0.01	0.30 ± 0.02	NaCl type structure [a]
	1.01 ± 0.01	0.016 ± 0.002	NaCl type structure [a]

[a] NbO like structure which is very similar to VO structure.

$V_2O_5 + Nb_2O_5$ respectively at 923 K for 4 weeks. For the doped VO sample, the metal ratio Nb/(V + Nb) was determined by means of X-ray fluorescence analysis. The phases of the samples were determined by X-ray diffractometry, and the results are given in Table 1.

Heat capacity measurement

Heat capacity was measured with an adiabatic scanning calorimeter [10]; in this calorimeter, the power supplied to the sample was measured continuously and the heating rate was kept constant during the measurements regardless of the kind and amount of sample. The heating rate was chosen to be 2 K min^{-1} for most samples except $VO_{1.063}$ and both 2 K min^{-1} and 1 K min^{-1} were chosen for $VO_{1.267}$. The heat capacity measurement was carried out from 323 to 920 K under a pressure of ca. 130 Pa. The crushed sample was sealed in a quartz vessel filled with helium gas at about 20 kPa. The amount of sample used for the measurement was about 13 g for each experiment. The heat capacity measurement was conducted within an imprecision of $\pm 3\%$.

RESULTS AND DISCUSSION

Heat capacity

Low temperature heat capacity anomaly

The results of the heat capacity measurements on $VO_{1\pm x}$ (O/V ratio = 0.883, 1.063 and 1.267) are shown in Fig. 1 together with that for VO reported by Orr [9]. Two heat capacity anomalies are seen in the figure. One is seen in all samples of $VO_{0.883}$, $VO_{1.063}$ and $VO_{1.267}$ in the temperature range between room temperature and 600 K (we designate it the low temperature heat capacity anomaly in this paper), where a steeper decrease in the heat capacity curve below about 450 K than the normal temperature dependence of the heat capacity under the equilibrium condition and a broad peak are seen; the other is seen in $VO_{0.883}$ and $VO_{1.063}$ around 900 K (we designate it the high temperature heat capacity anomaly), where one peak is generally attributed to the phase transition. The heat capacity values of $VO_{1.063}$ in the range 600–800 K between the low and the high temperature heat capacity anomalies in this study are close to those of VO determined with a drop calorimeter by Orr [9]. The results of the heat capacity measurements on Nb doped VO_{1+x} ($VO_{0.70}Nb_{0.30}O_{1.02}$ and $VO_{0.98}Nb_{0.02}O_{1.01}$) are shown in Fig. 2 in comparison with that for undoped $VO_{1.063}$. In the figure, both the low and the high temperature heat capacity anomalies are seen also in Nb doped VO_{1+x}. A similar low temperature heat capacity anomaly has been found in our laboratory for some of the V–O solid

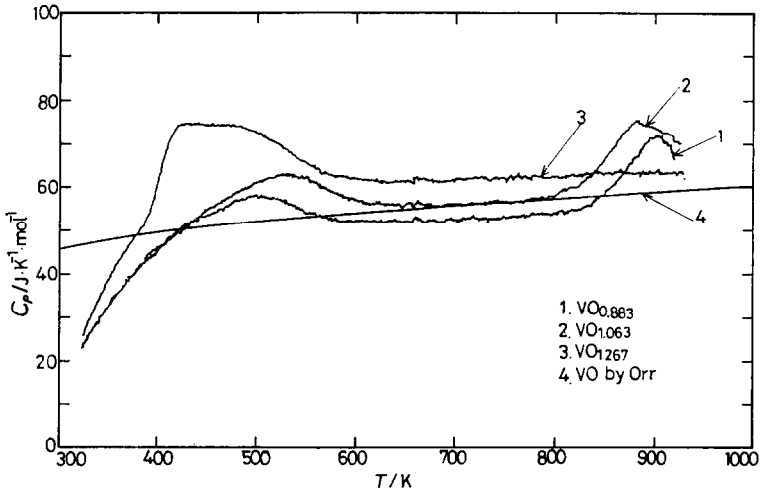

Fig. 1. Heat capacity of $VO_{1\pm x}$: 1: $VO_{0.883}$, 2: $VO_{1.063}$, 3: $VO_{1.267}$, 4: VO from Orr [9].

solutions (β'-VO_x: $x = 0.23$–0.25) [12] and Ti–O solid solutions (α-TiO_x: $x = 0.22$–0.47) [13], both of which have an order–disorder transition at high temperature. The presence of an order–disorder transition at about 1073 K in VO_{1+x} ($x = 0.2$–0.3) has been reported by Andersson and coworkers [3,14] and by Morinaga and Cohen [4]. Sato and coworkers also found experimentally two peaks in the heat capacity curve of FeCo [15] and Mg_3Cd [16], each of which have an order–disorder transition at high temperature. They analysed theoretically the kinetics of the order–disorder transition in the intermetallic alloys and showed the appearance of a second

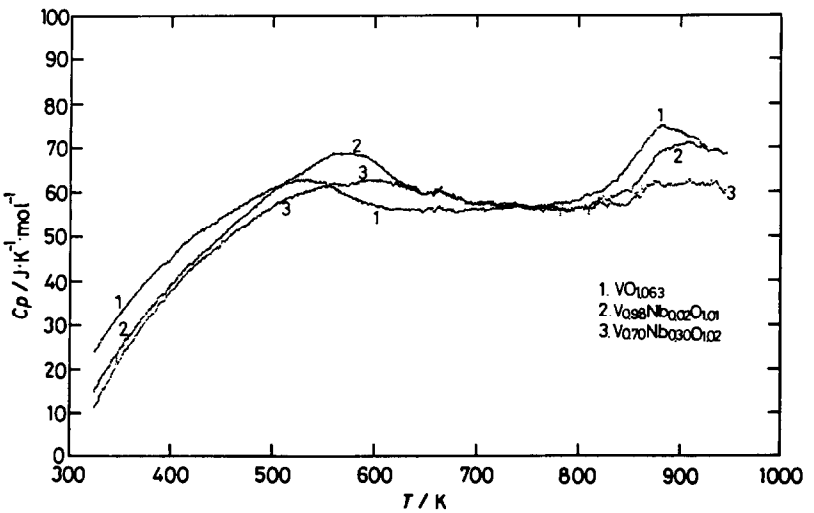

Fig. 2. Heat capacity of $VO_{1.063}$, $VO_{0.70}Nb_{0.30}O_{1.02}$ and $V_{0.98}Nb_{0.02}O_{1.01}$.

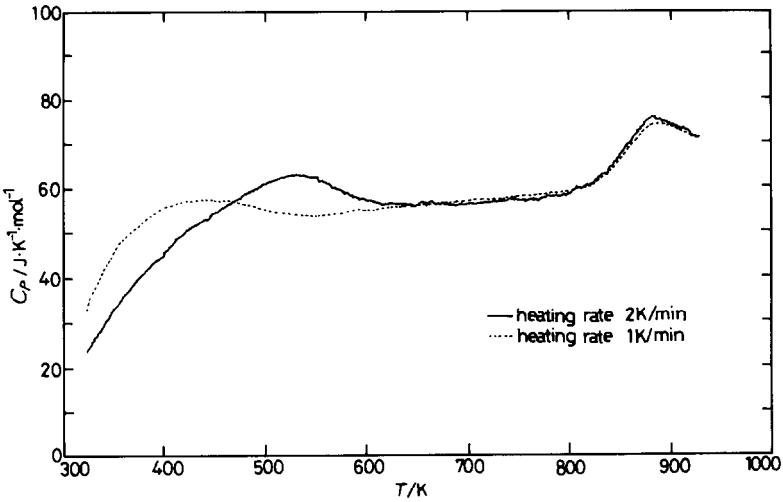

Fig. 3. Heat capacity of $VO_{1.063}$ measured at different heating rates: 2 K min^{-1} and 1 K min^{-1}.

peak in the heat capacity curve at the lower temperatures than the order–disorder transition temperature due to the "frozen in" phenomenon of long range order in addition to the peak of the order–disorder transition at high temperature. According to their theoretical analysis, the low temperature heat capacity anomalies observed for all samples of $VO_{1\pm x}$ and $(V,Nb)O_{1+x}$ in this study can be interpreted as follows. During cooling of the sample down to room temperature, the degree of long range order of the sample is frozen in at some temperature above room temperature but below the order–disorder transition temperature. When the temperature of such a sample with a lower degree of order than the equilibrium one at room temperature is raised, the atomic migration starts to induce an increase in the degree of order of the "frozen in" state at some temperature. This ordering process is exothermic and therefore the heat capacity obtained is lower than the equilibrium value. With further heating, the degree of order of the sample becomes higher than the equilibrium one because of the time lag of atomic migration. These processes are thought to produce an anomalous low temperature heat capacity rise at first, then the endothermic disordering process starts to produce a broad peak in the heat capacity, appearing below the main peak at the order–disorder transition temperature. The result for the effect of the heating rate on the low temperature heat capacity anomaly of $VO_{1.063}$ is shown in Fig. 3. It is seen in the figure that the low temperature heat capacity anomaly decreases as the heating rate decreases, indicating the validity of the application of the theory proposed by Sato and coworkers to $VO_{1\pm x}$ samples.

The doping effect of Nb in VO_{1+x} on the low temperature heat capacity anomaly is seen in Fig. 2. The heat capacity of doped VO_{1+x} below 500 K is

smaller than that of undoped $VO_{1\pm x}$. The peak temperature of the low temperature heat capacity anomaly is increased by Nb doping in VO_{1+x}. Since the X-ray diffraction patterns of VO_{1+x} doped with Nb ($V_{0.98}Nb_{0.02}O_{1.01}$ and $V_{0.70}Nb_{0.30}O_{1.02}$) were observed to be more similar to that of NbO type structure with both ordered cation and anion vacancies [17] than to the VO type structure, the more ordered arrangement in $(V, Nb)O_{1+x}$ may retard the recovery of the degree of order of the "frozen in" state, and results in the increase of the peak temperature of the low temperature heat capacity anomaly.

High temperature heat capacity anomaly

The heat capacity anomaly at high temperature, around 900 K, is seen in $VO_{1\pm x}$ and $(V,Nb)O_{1+x}$ except for $VO_{1.267}$ in Figs. 1 and 2. It is thought that this heat capacity anomaly is due to the order–disorder rearrangement of clusters of oxygen and vanadium vacancies and/or clusters of interstitial vanadium and vanadium vacancy, as was described in relation to the low temperature heat capacity anomaly. The heat capacity anomaly may also exist in $VO_{1.267}$ at higher temperature, above 920 K, than the experimental temperature range covered in this study, since the presence of the order–disorder transition around 1073 K in $VO_{1.23}$ has been reported by Høier and Andersson from studies by electron diffractometry [14].

The heat capacity of $VO_{1\pm x}$, C_p, is expressed by the sum

$$C_p = C_h + C_d + C_{ah} + C_e + \Delta C \tag{1}$$

where C_h is the harmonic term of the lattice vibration, C_d is the dilational term, C_{ah} is the anharmonic term of the lattice vibration, C_e is the electronic term, and ΔC is the excess heat capacity due to order–disorder transition. Hence the excess heat capacity ΔC can be obtained by subtracting the terms C_h, C_d, C_{ah} and C_e from the measured heat capacity C_p.

The harmonic term of the lattice vibration was estimated from the temperature dependence of the heat capacity of $VO_{1\pm x}$at low temperatures reported by Chernyaev et al. [8]. The Debye temperatures θ_D for $VO_{0.883}$, $VO_{1.063}$ and $VO_{1.267}$ calculated by the present authors, based on the low temperature heat capacity data of Chernyaev et al. [8], are 582, 595 and 585 K, respectively. The harmonic molar heat capacity for $VO_{1\pm x}$ can be expressed as

$$C_h = 3RD(\theta_D/T)(1 + O/V) \tag{2}$$

where $D(\theta_D/T)$ is the Debye function.

The dilational term of the molar heat capacity C_d can be expressed as

$$C_d = (V_m\beta^2/\alpha)T \tag{3}$$

where β is the thermal isobaric expansivity, V_m is the molar volume, and α is the isothermal compressibility. The values of $\beta = 2.81 \times 10^{-5}$ and $\alpha =$

6.38×10^{-6} cm^3 J^{-1} measured for $VO_{1.0}$ by Taylor and Doyle [18,19] were used for the calculation of C_d for all samples $VO_{0.882}$, $VO_{1.062}$ and $VO_{1.267}$ without considering the compositional differences. The molar volume was calculated from the lattice constants for $VO_{0.882}$, $VO_{1.063}$ and $VO_{1.267}$ at room temperature reported by Banus and Reed [1]. The following equations were obtained

$$C_d(\text{J K}^{-1}\ \text{mol}^{-1}) = 1.23 \times 10^{-3}\ T\ (\text{K}) \text{ for } VO_{0.882} \quad (4)$$

$$C_d = 1.28 \times 10^{-3}\ T \text{ for } VO_{1.062} \quad (5)$$

$$C_d = 1.32 \times 10^{-3}\ T \text{ for } VO_{1.267} \quad (6)$$

No data to estimate the anharmonic and electronic terms of the molar heat capacity of $VO_{1\pm x}$ are available. In the present calculation the excess heat capacity (ΔC) due to order–disorder transition is assumed to be negligibly small in the temperature range 650–800 K for $VO_{0.883}$ and $VO_{1.063}$ and above 650 K for $VO_{1.267}$, since the heat capacity values of $VO_{1.063}$ in this temperature range (650–800 K) are close to those of VO previously determined with a drop calorimeter by Orr [9]. The anharmonic and electronic

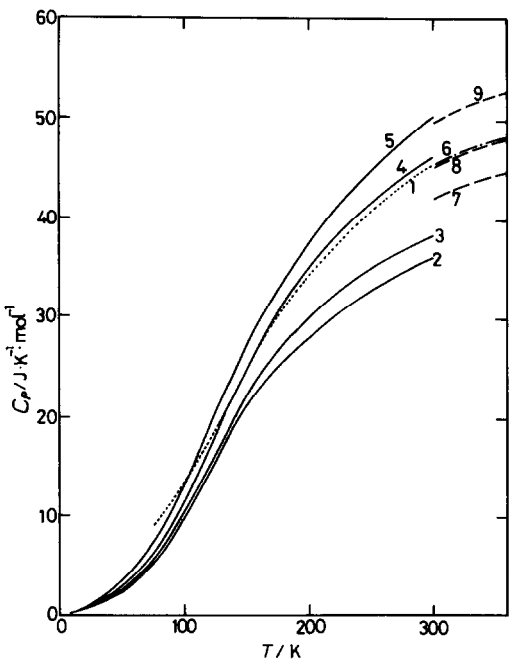

Fig. 4. Heat capacity of $VO_{1\pm x}$ at low temperatures; 1: VO from Todd and Bonnickson [7], 2: $VO_{0.86}$ by Chernyaev et al. [8], 3: $VO_{0.99}$ by Chernyaev et al. [8], 4: $VO_{1.24}$ from Chernyaev et al. [8], 5: $VO_{1.30}$ by Chernyaev et al. [8], 6: $VO_{1.0}$ from Orr [9], 7: $VO_{0.883}$ estimated from the base-line heat capacities in this study, 8: $VO_{1.063}$ estimated in this study, 9: $VO_{1.267}$ estimated in this study.

terms were then calculated from the experimental heat capacity values in such temperature ranges as the following

$$C_p - C_h - C_d = C_{ah} + C_e = (b + \gamma)T \tag{7}$$

where b is the coefficient of anharmonic heat capacity and γ is the coefficient of the high temperature electronic heat capacity. The sums of the coefficients $b + \gamma$ for $VO_{0.882}$, $VO_{1.063}$ and $VO_{1.267}$ are 7.8×10^{-3}, 6.8×10^{-3} and 6.6×10^{-3} J K^{-2} mol^{-1}, respectively.

The base-line heat capacities of $C_h + C_d + C_{ah} + C_e$ of $VO_{0.883}$, $VO_{1.063}$ and $VO_{1.267}$ thus obtained in this study were extrapolated to the low temperature region around 300 K and in Fig. 4 are compared with the heat capacities of $VO_{1\pm x}$ at low temperature, below 300 K, reported by other researchers [7–9]. It is seen in the figure that the heat capacity of $VO_{1.063}$ at 300 K estimated in this study is in good agreement with those of $VO_{1.0}$ reported by Todd and Bonnickson [7] and Orr [9].

The excess heat capacities C for $VO_{0.883}$ and $VO_{1.063}$ at the order–disorder transition temperature were estimated from the difference between the experimental values and the base-line of $C_h + C_d + C_{ah} + C_e$. By integrating the excess heat capacity up to 920 K, which is the highest temperature measured in this study, the changes in enthalpy (ΔH_t) and entropy (ΔS_t) for $VO_{0.883}$ and $VO_{1.063}$ at the phase transition were calculated, and the results are shown in Table 2.

The entropy change due to the order–disorder transition, on the other hand, can be calculated theoretically based on the defect structure reported by Morinaga and Cohen [4,5], who proposed the presence of two types of defect clusters for $VO_{1\pm x}$: one is composed of oxygen and vanadium vacancies (cluster A) mainly in the hypostoichiometric region and the other is the tetrahedron consisting of the interstitial vanadium ion and vanadium vacancies (cluster B) predominantly in the hyperstoichiometric region. In the present calculation for the entropy change, both clusters A and B are assumed to be present in both hypo- and hyperstoichiometric regions. For

TABLE 2

Transition temperature and the enthalpy and entropy changes of $VO_{1\pm x}$ at the transition obtained experimentally

O/V ratio	Transition temp., T (K)	ΔH_t (J mol^{-1})	ΔS_t (J K^{-1} mol^{-1})
0.883	905	$(874 \pm 34) + \alpha$ [a]	$(0.99 \pm 0.04) + \alpha$ [a]
1.063	883	$(1112 \pm 44) + \alpha$ [a]	$(1.26 \pm 0.06) + \alpha$ [a]

[a] The heat capacity anomalies are not completed at 920 K, which is the highest temperature measured in this study.

cluster A in the hypostoichiometric region ($NV_v < NO_v$), the configurational entropy change is calculated as

$$S_1 = k \ln \frac{(NO_v)!}{(NV_v)!(NO_v - NV_v)!}$$

$$\approx kN\{O_v \ln[O_v/(O_v - V_v)] - V_v \ln[V_v/(O_v - V_v)]\} \quad (8)$$

where k is Boltzmann's constant, N is the number of the vanadium and oxygen lattice site, V_v is the atomic fraction of vanadium vacancy and O_v is the atomic fraction of oxygen vacancy. For cluster A in the hyperstoichiometric region ($NV_v > NO_v$),

$$S_1 = k \ln \frac{(NV_v)!}{(NO_v)!(NV_v - NO_v)!}$$

$$\approx kN\{V_v \ln[V_v/(V_v - O_v)] - O_v \ln[O_v/(V_v - O_v)]\}. \quad (9)$$

For cluster B in both hypo- and hyperstoichiomeric regions,

$$S_2 = k \ln \frac{(NV_v)!}{(4NV_i)!(NV_v - 4NV_i)!}$$

$$\approx kN\{V_v \ln[V_v/(V_v - 4V_i)] - 4V_i \ln[4V_i/(V_v - 4V_i)]\} \quad (10)$$

where V_i is the atomic fraction of vanadium interstitials. Using the values of V_v, O_v and V_i reported by Banus and Reed [1] and Andersson et al. [3] such as 0.123, 0.225 and 0.009, respectively, for $VO_{0.883}$, and 0.158, 0.105 and 0.035 for $VO_{1.063}$, the entropy changes were calculated and the results are shown in Table 3. The values of the entropy change for $VO_{0.883}$ and $VO_{1.063}$ obtained experimentally, as shown in Table 2, are small in comparison with those calculated theoretically from the defect structure and shown in Table 3. This difference may originate from two facts: (1) the heat capacity anomalies for both $VO_{0.883}$ and $VO_{1.063}$ are not completed at 920 K, which is the highest temperature used in this study, and (2) the assumption for the theoretical calculation that the disordering in the $VO_{1\pm x}$ phase is completed is not adequate, since the presence of local order of defects in $VO_{1\pm x}$ has

TABLE 3

Entropy change calculated theoretically assuming the order–disorder transition of the defect clusters

O/V ratio	ΔS_1 ($J\,K^{-1}\,mol^{-1}$)	ΔS_2 ($J\,K^{-1}\,mol^{-1}$)	ΔS_t [a] ($J\,K^{-1}\,mol^{-1}$)
0.883	1.29	0.62	1.91
1.063	0.84	0.90	1.74

[a] ΔS_t: total entropy change ($= \Delta S_1 + \Delta S_2$).

been reported to persist above the order–disorder transition temperature by Andersson and coworkers [6,14,20,21] and Morinaga and Cohen [5].

It is seen in Fig. 2 that the transition temperature is increased and the entropy change at the transition is decreased by doping Nb in VO_{1+x}. The reason for this change is not clear at present, but the entropy change due to the disordering of the clusters involving the interstitial vanadium ions at the transition may be decreased with the decrease of the content of interstitial vanadium ions by substituting Nb in VO_{1+x}, and the ordered structure can exist up to high temperature (even above 950 K) since the Nb doped VO_{1+x} phase has the NbO like structure, which is more stable than the $VO_{1.0}$ structure at high temperature.

Electrical conductivity

The electrical conductivities of $VO_{1.063}$ and $VO_{1.267}$ were measured under the condition of the same constant heating rate (2 K min^{-1}) as that for the heat capacity measurements. The electrical conductivities of $VO_{1.063}$ and $VO_{1.267}$ are shown as a function of the reciprocal temperature in Figs. 5 and 6, respectively. It is seen in Fig. 5 that the $VO_{1.063}$ phase (δ-phase) is semiconducting and the slope in the conductivity curve changes at about 540 K and 870 K, temperatures which are close to the peak temperatures ($\simeq$ 540 and 880 K) of the heat capacity anomalies. The semiconducting behavior of the $VO_{1\pm x}$ phase (δ-phase) has been observed at low temperatures below 500 K by some researchers [1,22,23] and is also expected from the similarity

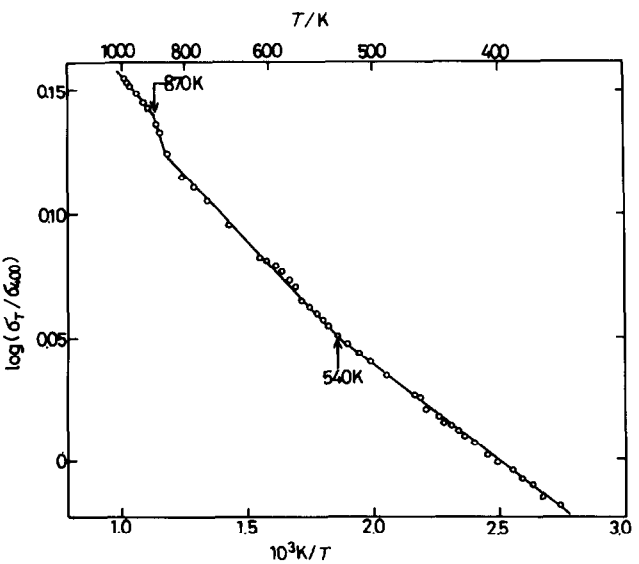

Fig. 5. Electrical conductivity of $VO_{1.063}$.

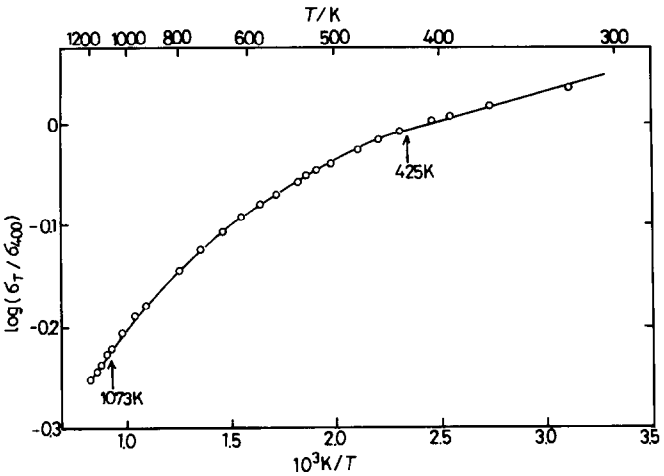

Fig. 6. Electrical conductivity of $VO_{1.267}$.

of the defect structure of VO_x ($x > 1$) to that of semiconductor Fe_xO [5]. The electrical conductivity of $VO_{1.267}$ (ϵ-phase) was first measured in this study. It is seen in Fig. 6 that the $VO_{1.267}$ phase is a metallic conductor and the slope changes at about 425 K from linear to non-linear; this temperature is in good agreement with the peak temperature ($\simeq$ 425 K) of the low temperature heat capacity anomaly, although the slope change is not so clear. The presence of the order–disorder transition at about 1073 K in the tetragonal VO_{1+x} phase (ϵ-phase) reported by Andersson and coworkers [3,14] and by Morinaga and Cohen [4] was not clearly confirmed from the electrical conductivity measurement in this study. The metallic property may come from the overlapping of the 3*d* conduction band produced by the contraction in the *c*-axis direction of the tetragonal ϵ-phase.

CONCLUSIONS

(1) The heat capacity anomaly was first observed at about 900 K in the δ-$VO_{1\pm x}$ phase ($VO_{0.883}$ and $VO_{1.063}$). The heat capacity anomaly was considered to be due to the order–disorder transition of the clusters composed of (A) vanadium vacancy and oxygen vacancy, and (B) the tetrahedron of interstitial vanadium ion and vanadium vacancies. The entropy change at the transition was calculated based on the disordering of these two kinds of defects and compared with the experimental values. The presence of the transition was also confirmed by the electrical conductivity measurement.

(2) The presence of the order–disorder transition in $VO_{1.267}$ (ϵ-phase) relating to the defect clusters at about 1073 K, which has been observed by

X-ray diffraction, was not clearly confirmed by the electrical conductivity measurement in this study.

(3) For the order–disorder transition at high temperature, the transition temperature was increased and the enthalpy change at the transition was decreased by doping Nb in VO_{1+x}.

(4) In the temperature range lower than the temperature of the order–disorder transition, a heat capacity anomaly was also observed. The low temperature heat capacity anomaly was thought to originate from the relaxation process of the order of the "frozen in" state by atomic migration.

(5) The base-line of the heat capacity, $C_h + C_d + C_{ah} + C_e$ was evaluated. The heat capacity of $VO_{1.063}$ at 300 K estimated by the base-line was in good agreement with those of $VO_{1.0}$ reported by Todd and Bonnickson [7] and by Orr [9].

(6) From the electrical conductivity measurement, the δ-$VO_{1\pm x}$ phase ($VO_{1.063}$) was confirmed as being a semiconductor, as was expected from the literature [1,22,23]. The electrical conductivity of the ϵ-VO_{1+x} phase ($VO_{1.267}$) was first measured and metallic behavior was found.

ACKNOWLEDGEMENTS

The authors thank Dr. M. Iseki for the use of a plasma jet furnace. The authors are also indebted to Professors D. Ishii, K. Sugiyama and T. Takeuchi of Nagoya University for the use of the X-ray fluorescence analyzer.

REFERENCES

1 M.D. Banus and T.B. Reed, in L. Eyring and M. O'Keefe, (Eds), The Chemistry of Extended Defects in Non-Metallic Solids, North-Holland, Amsterdam, 1970, p. 488.
2 M. Saeki and M. Nakahira, Mater. Res. Bull., 6 (1971) 603.
3 B. Andersson, J. Gjonnes and A.R. Forouhi, J. Less-Common Met., 61 (1978) 273.
4 M. Morinaga and J.B. Cohen, Acta Crystallogr., Sect. A, A35 (1979) 745.
5 M. Morinaga and J.B. Cohen, Acta Crystallogr., Sect. A, A35 (1979) 975.
6 B. Andersson and J. Gjönnes, Acta Chem. Scand., 24 (1970) 2250.
7 S.S. Todd and K.R. Bonnickson, J. Am. Chem. Soc., 73 (1951) 3894.
8 V.S. Chernyaev, E. N. Shchetnikov and P.V. Gel'd, Tr. Ural. Politekh. Inst., (167) (1968) 151.
9 R.L. Orr, J. Am. Chem. Soc., 76 (1954) 857.
10 K. Naito, H. Inaba, M. Ishida, Y. Saito and H. Arima, J. Phys. E 7 (1974) 464.
11 K. Naito, T. Tsuji and T. Matsui, J. Nucl. Mater., 48 (1973) 58.
12 K. Naito, H. Inaba and S. Tsujimura, 1979, unpublished work.
13 T. Tsuji, M. Sato and K. Naito, Thermochim. Acta, to be published.
14 R. Høier and B. Andersson, Acta Crystallogr., Sect. A, A30 (1974) 93.
15 H. Sato and R. Kikuchi, Acta Metall., 24 (1976) 797.

16 K. Gsckwend, H. Sato, R. Kikuchi, H. Iwasaki and H. Maniwa, J. Chem. Phys., 71 (1979) 2844.
17 G. Brauer, Z. Anorg. Allg. Chem., 248 (1941) 1.
18 A. Taylor and N.J. Doyle, J. Appl. Crystallogr., 4 (1971) 103.
19 A. Taylor and N.J. Doyle, J. Appl. Crystallogr., 4 (1971) 109.
20 D. Watanabe, B. Andersson and J. Gjönnes, Acta Crystallogr., Sect. A, A30 (1974) 772.
21 B. Andersson, J. Gjönnes and J. Taft , Acta Crystallogr., Sect. A, A30 (1974) 216.
22 S. Takeuchi and K. Suzuki, Nippon Kinzoku Gakkaishi, 31 (1967) 611.
23 S. Kawano, K. Kosuge and S. Kachi, J. Phys. Soc. Jpn., 21 (1966) 2744.